Author/s:
Vaz, PK;Armat, M;Hartley, CA;Devlin, JM

Title:
Codon pair bias deoptimization of essential genes in infectious laryngotracheitis virus reduces protein expression

Date:
2023-01-01

Citation:
Vaz, P. K., Armat, M., Hartley, C. A. & Devlin, J. M. (2023). Codon pair bias deoptimization of essential genes in infectious laryngotracheitis virus reduces protein expression. Journal of General Virology, 104 (4), https://doi.org/10.1099/jgv.0.001836.

Persistent Link:
https://hdl.handle.net/11343/333235

JOURNAL OF GENERAL VIROLOGY

RESEARCH ARTICLE

Vaz *et al.*, *Journal of General Virology* 2023;104:001836

DOI 10.1099/jgv.0.001836

MICROBIOLOGY SOCIETY

OPEN ACCESS

Codon pair bias deoptimization of essential genes in infectious laryngotracheitis virus reduces protein expression

Paola K. Vaz*, Marzieh Armat, Carol A. Hartley† and Joanne M. Devlin†

Abstract

Infectious laryngotracheitis virus (ILTV; an alphaherpesvirus) is a respiratory pathogen of chickens and causes significant economic losses in the poultry industry globally, in addition to severe animal health and welfare concerns. To date, studying the role of ILTV genes in viral infection, replication or pathogenesis has largely been limited to genes that can be deleted from the ILTV genome and the resultant deletion mutants characterized *in vitro* or *in vivo*. However, this approach is not suitable for the study of essential genes. This study trialled two different codon deoptimization techniques that aimed to separately disrupt and downregulate the expression of two ILTV genes, ICP8 and UL12, which are essential or very important in viral replication. The target genes were partially recoded using codon usage deoptimization (CUD) and codon pair bias deoptimization (CPBD) approaches and characterized *in vitro*. Viruses deoptimized via CPBD showed decreased protein expression as assessed by Western blotting and/or fluorescence microscopy to measure the intensity of the fluorescent marker fused to the target protein. Viruses deoptimized by CUD showed less consistent results, with some mutants that could not be generated or isolated. The results indicate that CPBD is an attractive and viable tool for the study of essential or critically important genes in ILTV. This is the first study, to our knowledge, that utilizes CPBD and CUD techniques for the study of ILTV genes.

INTRODUCTION

Gallid alphaherpesvirus 1 (infectious laryngotracheitis virus, ILTV) is a dsDNA virus that causes severe respiratory disease in chickens. The virus is horizontally transmitted through aerosols and fomites. Live attenuated ILTV vaccines are widely used in the poultry industry. Recombination involving attenuated vaccine strains has resulted in the generation of virulent recombinant viruses that have displaced other field viruses and caused outbreaks of disease. Full genome sequencing and recombination studies have highlighted ILTV's high genomic plasticity [1, 2].

Studying the role of herpesvirus genes in viral infection, replication and pathogenesis is aided by the generation of targeted gene mutants, including gene-deletion mutants. Herpesvirus genes can be classified as essential or non-essential for virus replication *in vitro*, through the construction of specific gene-deficient variants. Deletion of non-essential genes results in viruses that can be cultured and directly compared to the parent to study the functional role of the deleted genes. Deletion of essential genes results in non-viable viruses that cannot be cultured, and this limits functional characterization of the gene beyond its essential role. While for many other herpesviruses the construction of bacterial artificial chromosomes (BACs) has facilitated the manipulation and study of essential or quasi-essential viral genes, BAC construction has not been successful for ILTV [3]. The ILTV genome encodes 80 ORFs, but the functions of most of these have not been characterized and ILTV gene function studies have largely been limited to non-essential genes. Specifically, gene-deletion studies have been limited to ORFs A–E, UL0, UL10, UL21, UL47, UL49.5, UL50, thymidine kinase (TK), and genes encoding glycoproteins C, G, E, I and J (gC, gG, gE, gI and gJ, respectively)

Received 27 November 2022; Accepted 02 March 2023; Published 03 April 2023

Author affiliations: [1]Asia-Pacific Centre for Animal Health, Melbourne Veterinary School, University of Melbourne, Parkville, Victoria, Australia.

***Correspondence:** Paola K. Vaz, pvaz@unimelb.edu.au

Keywords: codon deoptimization; ICP8; ILTV; recombination; UL12.

Abbreviations: BAC, bacterial artificial chromosome; CAI, codon adaptive index; CEK, chicken embryo kidney; CPB, codon pair bias; CPBD, codon pair bias deoptimization; CUD, codon usage deoptimization; d.p.i., days post-infection; ENC, effective number of codons; h.p.i., hours post-infection; ILTV, infectious laryngotracheitis virus; LMH, leghorn male hepatoma; qRT-PCR, quantitative reverse transcription PCR; sfGFP, superfold GFP; SNP, single nucleotide polymorphism.

The GenBank/EMBL/DDBJ accession numbers for the viral genome sequences are CSW1, OQ290763; CPBDh.ICP8, OQ290764; WT.ICP8, OQ290765; WT.UL12, OQ354886; CUDs.UL12, OQ354889; CPBDh.UL12, OQ354887; CPBDq.UL12, OQ354888.

†These authors contributed equally to this work

One supplementary figure, two supplementary tables and supplementary text are available with the online version of this article.

[4–15]. The generation of gene-deleted mutants has been central to studying the role of these genes in ILTV and has also been useful for generating targeted deletion-mutant vaccine candidates. However, the study of genes critically important for ILTV replication in cell culture requires a different approach.

In other viruses, two genomic recoding approaches have been utilized to disrupt protein expression of essential or quasi-essential genes: codon usage deoptimization (CUD) and codon pair bias deoptimization (CPBD) [16, 17]. CUD involves the substitution of the most preferred codons within a target ORF with those of the least favourable codons for a specific animal host. CPBD is based on the observation that some codon pairs occur more or less frequently in some viral genomes compared to the expected overall frequency of those two codons forming pairs within that host. CPBD involves the modification of this frequency [18, 19] and is often accompanied by an increase in CpG dinucleotide frequencies. Both codon deoptimization techniques work by slowing translation of encoded genes, resulting in reduced but not ablated expression of protein. Codon deoptimization has been widely used for RNA virus attenuation [18–20], while few studies have applied this technique to large dsDNA viruses [21–23]. Neither approach (CUD nor CPBD) has been previously applied to ILTV.

In this study, we explore both methodologies for the study of essential or important ILTV genes. Specifically, we applied CUD and CPBD to ILTV infected cell protein 8 (ICP8; UL29) and UL12 genes. In other alphaherpesviruses, these conserved proteins have important roles in viral replication and recombination [24, 25].

METHODS

Cells

The cells used in this study for viral propagation and characterization were leghorn male hepatoma (LMH) cells [26]. Chicken embryo kidney (CEK) cells were also utilized for selected virus propagation (V1-99) and characterization assays as previously described [27].

Viruses

The ILTV parent strain CSW1 was used in this study to construct viruses with deoptimized ORFs. This is a historical class 4 field isolate that has been used previously to generate various gene-deficient viruses, including a live attenuated vaccine [28, 29]. The strain V1-99 is a class 2 isolate used as the coinfecting virus to assess recombination through *in vitro* assays. Both viruses have been used previously to estimate ILTV recombination rates *in vivo* [30–32]. They share 99.8% nucleotide pairwise identity across their genomes, as well as similar growth kinetics in LMH cells [27, 30].

Recoding of ILTV UL12 and ICP8 (UL29) genes by CPBD and CUD

CPBD of the second half of the ILTV ICP8 ORF and the first half of the UL12 ORF was performed. Each CSW1 ICP8 and UL12 coding sequence (GenBank accession no. JX646899) was divided into quarters. The third and fourth quarters of the ICP8 gene, and the first and second quarters of the UL12 gene, were deoptimized using the Python script CodonShuffle [33] adapted to use the Echick.cut codon adaptive index (CAI) file within EMBOSS and the *Gallus gallus* codon pair scores (CPSs) published previously [34]. One thousand iterations were performed and the final CPBD sequences used in this study were selected based on their maximally decreased codon pair bias (CPB) score whilst maintaining CAI, effective number of codons (ENC) and minimum free energy (VFOLD) values that were similar or identical to CSW1 wild-type native ORF sequence. Sequences with increased CpG scores were also favoured (Table 1, Fig. 1, Supplementary Text, available with the online version of this article).

CUD of ICP8 and UL12 gene quarters was initially performed manually using the Integrated DNA technologies (IDT) optimization tool (https://sg.idtdna.com/pages/tools/codon-optimization-tool), with the *G. gallus* codon usage table as a reference to manually select sub-optimal codons per amino acid residue. Sequences were subsequently analysed using CodonShuffle as above to compare values to native CSW1 ORF sequences. One thousand iterations were performed in order to identify sequences with the lowest possible differences in CAI and ENC values compared to WT, without overly optimizing or deoptimizing CPB values and VFOLD values (Table 1, Fig. 1, Supplementary Text).

Repair plasmids were prepared by synthesis of recoded half gene sequences (IDT), followed by subcloning into pcDNA3.1(+) plasmid vector. All three ICP8 repair plasmids were designed to express the ICP8 fused to a superfold GFP (sfGFP) tag [35] in the C-terminus, whilst UL12 repair plasmids were designed to express the UL12 protein fused to sfGFP in the N-terminus to avoid disrupting the overlapping downstream UL11 ORF. As the fusion of a sfGFP tag to viral essential proteins may hinder virus replication, repair plasmids containing the sfGFP sequence along with either the wild-type sequence of CSW1 ICP8 or the wild-type sequence of CSW1 UL12 were constructed (Genscript) in order to isolate the effect of recoding. Each repair plasmid was linearized prior to co-transfection by restriction endonuclease digestion. See Table 2 for full list of constructs.

Table 1. Sequence features for each quartile of the ILTV ICP8 and UL12 genes in wild-type virus and in virus sequences that were CPBD and CUD recoded

Sequence values were obtained using the CodonShuffle sequence analyser tool.

Sequence	CPB	CG	mfe	ENC	CAI	No. of nt
ICP8						
CSW1 (wt)-Q3	−0.016	0.79	−224.2	55.11	0.71	882
CSW1 (wt)-Q4	−0.070	0.76	−251.2	57.84	0.72	882
CPBD Q3	−0.082	0.95	−224.2	55.07	0.71	–
CPBD Q4	−0.134	0.81	−251.2	57.77	0.72	–
CUD Q3	−0.017	0.85	−194.1	42.96	0.65	–
CUD Q4	−0.058	1.34	−233.9	44.64	0.59	–
UL12						
CSW1 (wt)-Q1	−0.072	1.106	−92.9	49.1	0.68	393
CSW1 (wt)-Q2	−0.044	0.9	−97.9	53.22	0.72	393
CPBD Q1	−0.102	1.166	−92.9	49.22	0.68	–
CPBD Q2	−0.098	0.981	−97.9	53.14	0.72	–
CUD Q1	−0.08	2.37	−88.5	22.43	0.46	–
CUD Q2	−0.05	2.31	−195.6	22.78	0.49	–

mfe, minimum free energy.

Construction of ILTV ICP8 and UL12 half deoptimized mutants by co-transfection experiments

Viral genomic DNA was extracted from CSW1-infected cell cultures as described elsewhere [36], with minor modifications. Co-transfection experiments were performed by incubating ~2 µg viral genomic DNA, 2 µg linearized repair plasmid, 2 µg pICP4 plasmid and 12 µl X-tremeGENE HP DNA transfection reagent (Sigma) in Dulbecco's Modified Eagle Medium (DMEM) for 20 min at room temperature, according to manufacturer's instructions. A 200 µl aliquot of these solutions was applied to sub-confluent monolayers of LMH cells in 6-well trays. Three days after co-transfection, green fluorescent plaques were identified using fluorescence microscopy, collected by micropipette and stored at −80 °C. Further plaque purification (at least three rounds)

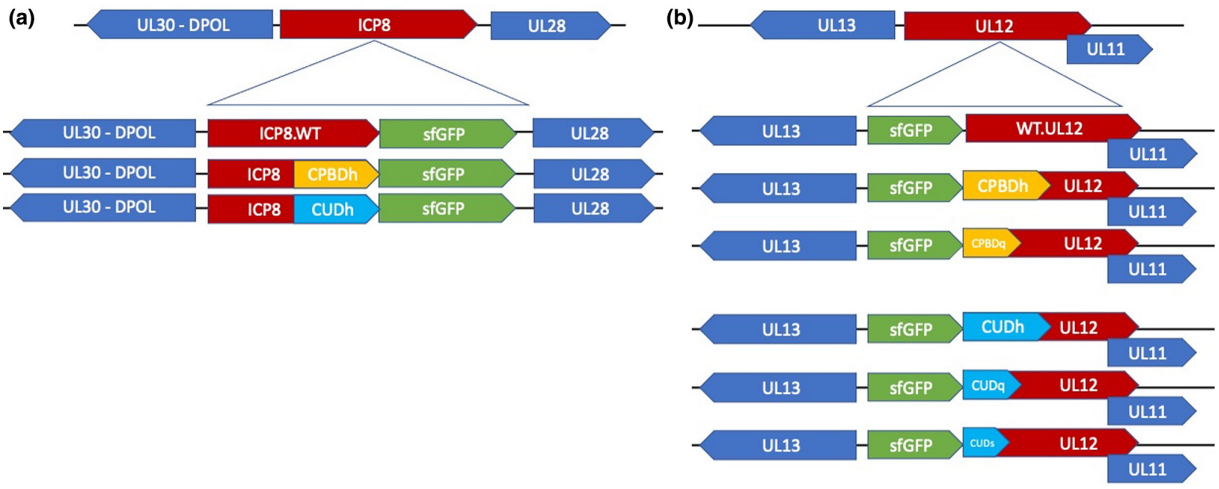

Fig. 1. Schema of insertion designs for the recoded ILTV gene mutants generated via homologous recombination. (a) Designs for the ICP8 mutants, including WT ICP8 with sfGFP, and mutants with half of the ICP8 gene recoded using either CPBD or CUD, plus sfGFP. (b) Designs for the UL12 mutants, including WT UL12 with sfGFP, and mutants with a sixth, quarter or half of the UL12 gene recoded using CPBD or CUD, plus sfGFP.

Table 2. Panel of sfGFP-tagged CSW1-derived mutants targeted for this study, indicating the deoptimization approach used to recode them

Deoptimization approach	Target gene	Proportion of gene recoded	Expected virus recovered	Outcome	Resulting virus construct name
None	ICP8	0	Yes	Wild-type ICP8	WT.ICP8
	UL12	0	Yes	Wild-type UL12	WT.UL12
Codon usage (CUD)	ICP8	0.5	No	–	–
	UL12	0.5	No	Recovered virus with 1/6th recoded UL12	CUDs.UL12
	UL12	0.25	No		
Codon pair bias (CPBD)	ICP8	0.5	Yes	Half recoded ICP8	CPBDh.ICP8
	UL12	0.5	Yes	Half recoded UL12	CPBDh.UL12
	UL12	0.25	Yes	Quarter recoded UL12	CPBDq.UL12

was performed until no WT (non-fluorescent) virus was detected by microscopy or by PCR. Sanger sequencing of insertion sites and upstream and downstream regions was performed using BigDye Terminator mix (ThermoFisher Scientific) at the Australian Genome Research Facility. Final stocks of each plaque-purified virus containing the recoded sequences were amplified and viral genomes sequenced using Illumina next generation NovaSeq short-read chemistry (Illumina) at Charles River Laboratories. Genome assemblies were performed using both *de novo* and map to reference methodologies as previously described [1].

Assessment of protein levels by fluorescence intensity

The effect of recoding on ICP8 and UL12 protein expression was assessed by quantitative fluorescence microscopic analysis of infected cells. LMH cells were inoculated with sfGFP-tagged ICP8 and UL12 mutants at an m.o.i. of 0.0001 to 0.02, in triplicate, and 19 to 46 individual fluorescent plaques were imaged at 1 to 3 (ICP8 recoded viruses) or 2 to 4 (UL12 recoded viruses) days post-infection (d.p.i.) using a Leica DM500 microscope with a ×10 objective. Images were analysed using FIJI v2.1.0 [37]. Background was subtracted from the green channel and Triangle Dark threshold applied, despeckled and median points of fluorescence with a radius of 3 pixels were removed and a watershed binary filter applied. The mean and the maximum integrated density of fluorescence for each deoptimized viral plaque were then measured, where mean refers to the average pixel fluorescent intensity value within defined fluorescent foci per image, while maximum refers to the highest pixel fluorescent intensity value within those foci (https://imagej.nih.gov/ij/docs/guide/user-guide.pdf). Deoptimized viruses were compared to those sfGFP-tagged viruses that contained native ICP8 (WT.ICP8) or UL12 (WT.UL12) nucleotide sequences.

GFP expression was also evaluated by Western blot analysis of UL12 and ICP8 mutants at a single timepoint. LMH cells were inoculated with WT.UL12, CUDs.UL12 (sixth deoptimized), CPBDq.UL12 (quarter deoptimized), CPBDh.UL12 (half deoptimized), WT.ICP8 or CPBD.ICP8 isolates at an m.o.i. of 0.02 or were mock infected. Wells were harvested at 2 d.p.i. where lysates were collected into lysis buffer (2%, w/v, SDS, 10%, v/v, glycerol, 0.06 M Tris-HCl pH 6.8, 0.05 mM β-mercaptoethanol and 0.5 mg bromophenol blue ml^{-1}) and proteins separated in a 10% (w/v) acrylamide gel by SDS-PAGE under reducing conditions. Western blotting was performed probing with rat antiserum to ILTV gI or ILTV gD, or rabbit eGFP polyclonal antibody (ThermoFisher Scientific) as previously described [38], and virus sample loading was adjusted to ensure equivalent amounts of unmodified proteins (gI or gD) between samples to allow for comparison of GFP expression relative to another ILTV protein.

Assessment of gene transcript levels by quantitative Reverse Transcription-PCR (qRT-PCR)

To assess the impact of recoding on ICP8 and UL12 transcription, qRT-PCRs were performed on the recoded mutants and compared to WT GFP-labelled control virus (WT.ICP8 and WT.UL12, respectively). Confluent monolayers of LMH cells were inoculated with each recoded virus, WT.ICP8 and WT.UL12 at an m.o.i. of approximately 1, in triplicate. Residual inoculum was removed with a 0.2 M citrate buffer (40 mM citric acid, 10 mM KCl, 135 mM NaCl, pH 3.0) after 2 h at 37 °C, and fresh medium added (DMEM supplemented with 10%, v/v, FBS and 2 mM HEPES pH 7.4). Cultures were further incubated until 4 h.p.i. (hours post-infection), when supernatant was removed and cell lysates captured in RLT Plus buffer (Qiagen). RNA was extracted using the RNeasy Plus RNA isolation kit (Qiagen), as per the manufacturer's instructions. Eluates were subjected to DNase treatment using a Turbo DNase-free kit (ThermoFisher Scientific), according to the manufacturer's instructions. Complementary DNA was synthesized using Superscript III RT (ThermoFisher Scientific) according to the manufacturer's instructions, and 2 µl each cDNA template was tested using oligonucleotides targeting ILTV cDNA from ICP8 (F, 5′-GCCTCGAGCGGACTAACC-3′; R, 5′-GTTCGGGGCTAAAACCACAGG-3′), UL12 (F, 5′-CGCGATTTCTTGCTGGGAATTTC-3′; R, 5′-CTGTCAGTTTTCCAAG TTTTGTC-3′) and ICP4 (F, 5′-ACCTGTTGGCGGCTCTTAG-3′; R, 5′-CAGACGCCGCCGTAGGAT-3′). The relative expression

levels of ICP8 and UL12 transcripts were expressed as ΔΔCt [39], with the ICP8 and UL12 transcripts normalized against the viral ICP4 reference transcript and each recoded mutant against either WT.ICP8 or WT.UL12 virus.

Viral replication and cell-to-cell spread

To assess the effect of ICP8 and UL12 deoptimization on viral replication kinetics, a multi-step growth curve experiment was performed as previously described [40] with minor modifications. Briefly, each virus was inoculated onto sub-confluent LMH cells at an m.o.i. of approximately 0.001, in triplicate. Wells were harvested at 24 h timepoints for 4 days and stored at −70 °C, and each sample was subsequently titrated on LMHs cells to determine the viral titre by either $TCID_{50}$ [41] or p.f.u. ml^{-1} [27].

Cell-to-cell spread was compared between the two CSW1-derived ICP8 mutants (CPBDh.ICP8 and WT.ICP8) to that of the CSW1 parent virus. Sub-confluent monolayers of LMH cells in 6-well trays were infected with 50 and 100 p.f.u. of each virus, in duplicate. Twenty to thirty plaques per day were photographed and measured using ImageJ version 2.0 [37], as previously described [40].

In vitro coinfection recombination experiments

The impact of deoptimizing ICP8 expression on the capacity for ILTV viruses to recombine *in vitro* was evaluated through a coinfection assay. LMH cells were simultaneously coinfected with a total m.o.i. of 8 using the V1-99 ILTV strain with CSW1 parent and derivative mutants. Residual inoculum was removed with a 0.2 M citrate buffer (40 mM citric acid, 10 mM KCl, 135 mM NaCl, pH 3.0) after 1 h at 37 °C, and fresh medium added (DMEM supplemented with 5%, v/v, FBS and 2 mM HEPES pH 7.4). Infected wells were harvested after 24 h, serially diluted to 10^{-4} and used to inoculate LMHs cells within 6-well trays and covered by a 1% (w/v) methylcellulose overlay. Thirty isolated plaques from each coinfection were picked using only brightfield microscopy at 24 and 48 h.p.i., and the DNA extracted (MagMAX CORE nucleic acid purification kit; ThermoFisher Scientific). The picked progeny were then genotyped using a TaqMan single nucleotide polymorphism (SNP) genotyping assay that targets five sites within the genome where CSW1 and V1-99 vary [30]. Any plaques determined to contain a mixed signal phenotype by TaqMan probes at any SNP were excluded from further statistical analysis.

Statistical analysis

Statistical comparisons between the mutant viruses and the CSW1 parent, WT.ICP8 or WT.UL12 viruses were performed across the different phenotypic assays. Plaque area, viral titres and plaque fluorescence intensity were compared between viruses at each timepoint using two-way ANOVA followed by Tukey's Honest Significant Difference test. For comparison of gene transcript data, two-tailed Mann–Whitney tests were used to compare ΔΔCt values of mutant viruses to their respective parent viruses. The recombination rate of CPBDh.ICP8 and WT.ICP8 mutants was compared to that of the CSW1 parent and assessed by analysis of the proportion of recovered plaques that corresponded with either parent (CSW1 or V1-99) or recombinant genotype profiles using a Fisher's exact test. $P<0.05$ was considered significant.

RESULTS

CPBD, but not CUD, was successful in generating defined mutant viruses

A panel of viruses with CUD or CPBD recoded regions of ICP8 or UL12 were designed (Fig. 1, Table 1), and a summary of the viruses recovered is shown in Table 2. CPBD was successful in producing a panel of mutants for further characterization, while the application of CUD produced less consistent results since some viruses could not be either generated or isolated. Two ICP8 mutants (CPBDh.ICP8 and WT.ICP8) and four UL12 mutants (CPBDh.UL12, CPBDq.UL12, CUDs.UL12 and WT.UL12) were constructed by co-transfection, and plaque-purified at least three times in order to ensure the absence of CSW1 parent. These were further confirmed for the absence of parent by PCR. Neither of the CUD half mutants (CUDh.ICP8 and CUDh.UL12) nor the CUD quarter mutant (CUDq.UL12) could be cultured and purified in the absence of CSW1 wild-type parent on LMH or CEK cells. When quarter and half CUD recoded UL12 viruses were being developed, both pathways resulted in UL12 CUD mutants with identical partial deoptimization of the UL12 gene region. Specifically, only nucleotides 1–228 of the UL12 5' end was codon usage deoptimized as opposed to the targeted 1–393 (Q1) and 1–786 (half) regions, resulting in both mutagenesis experiments producing a 1/6th deoptimized UL12 ORF mutant (CUDs.UL12; Fig. 1, Table 2).

The genome sequencing results of the CSW1 parent and purified ICP8 mutants were compared. *De novo* assembly results were principally consistent with those produced by mapping against the reference sequence, with variation limited to regions rich in tandem repeats or secondary structure and, therefore, difficult to assemble with confidence. Several SNP variants were identified in the CSW1 parent that differed to the published CSW1 reference sequence (GenBank accession no. JX646899), and so subsequent comparisons of mutant genomes were limited to that of the study CSW1 parent (Table S1). Comparison of the two sequenced ICP8 mutants identified the presence of four (WT.ICP8) or two (CPBDh.ICP8) SNPs different from the parent CSW1 genome within coding sequences, excluding the expected ICP8 ORF recoding and sfGFP insertion.

Genome sequencing of UL12 deoptimized mutants identified some SNPs from CSW1, most notably SNPs in the ORF C gene in both CPBD mutants, that were predicted to result in premature truncation of this protein. As ORF C deficient ILTV constructs can impact plaque size phenotype though not replication efficiency [12], definitive assignment of phenotypic differences to UL12 gene deoptimization rather than ORF C truncation would not be possible for these viruses. As a result, UL12 deoptimized mutant characterization was limited only to replication and protein expression analyses as described below.

CPBD of partial UL12 and ICP8 gene sequences reduces protein expression

Plaque fluorescence intensity was used as a measure of ICP8 and UL12 protein expression in the mutants that encoded partially deoptimized coding sequences linked to sfGFP. CPBD ICP8 mutant (CPBDh.ICP8) plaques displayed significantly reduced mean fluorescence intensity compared to those of green fluorescent virus with a native ICP8 (WT.ICP8) sequence at 2 and 3 d.p.i. (Fig. 2a). Additionally, CPBDh.ICP8 viral plaques produced lower maximum fluorescence intensity across the 3 days measured (Fig. 2b, c). Both measures indicate decreased GFP signal accumulation within cells infected with CPBDh.ICP8 virus relative to those of WT.ICP8 regardless of plaque size. Mean fluorescence intensity values of UL12 deoptimized plaques were more variable, but both CPBD UL12 mutants showed a significant reduction in mean fluorescence intensity compared to WT.UL12 at 2, 3 and 4 d.p.i., and a reduced maximum fluorescence intensity compared to WT.UL12 at 3 d.p.i. with half deoptimized mutant displaying a lower maximum fluorescence intensity than the quarter deoptimized virus plaques (Fig. 2d, e). There was no significant difference in fluorescence intensity between the CUDs.UL12 and WT.UL12 viral plaques at any timepoint. Western blot analysis of GFP-tagged UL12 mutants at 2 d.p.i. demonstrated lower amounts of GFP produced in CPBD UL12 virus-infected LMH cells (relative to another unmodified ILTV protein, gI) compared to both WT.UL12 and CUDs.UL12 infected cells, consistent with observations from microscopic fluorescence analysis of these viruses (Fig. S1). In contrast, Western blot analysis of GFP-tagged ICP8 mutants did not detect reduced expression of GFP in CPBDh.ICP8 infected cells compared to WT.ICP8 infected cells (relative to another unmodified ILTV protein, gD), suggesting that the reduction in ICP8 expression may be too subtle to be detected by semi-quantitative Western blotting. The reduced fluorescence levels detected in CPBDh.ICP8 infected cells using microscopy techniques may also reflect the marked reduction in replication of this mutant compared to WT.ICP8 (Fig. 3a–c), which would result in reduced levels of GFP-tagged ICP8, and indeed all viral proteins.

Partial recoding of ICP8 and UL12 did not reduce gene transcript levels

ICP8 and UL12 transcription was assessed by qRT-PCR to determine whether modification of CPB or codon usage reduced target gene RNA transcripts relative to another unmodified ILTV viral gene (ICP4). This was performed in order to determine whether a reduction in transcription as a result of the recoding was the explanation for the reduced protein expression observed. Comparison of relative transcripts to WT GFP-tagged controls viruses indicated that neither CPBD nor CUD resulted in significantly reduced transcript levels for either ICP8 or UL12 (see Table S2).

ILTV mutants with CPBD UL12 or ICP8 gene sequences show altered viral growth characteristics in cell culture

Comparison of viral replication kinetics and plaque area indicated that CPBDh.ICP8 replicated at a lower rate over 4 days (Fig. 3a) and produced smaller plaques when compared to virus with the native ICP8 gene sequence (Fig. 3b). Plaques produced by CPBDh.ICP8 were 24–50% smaller than those produced by CSW1, and 44–56% smaller than WT.ICP8 plaques. These differences were statistically significant ($P<0.05$) at days 2 and 4 in the replication assay, and days 2 and 3 in the plaque area assay. Comparison of replication kinetics of codon deoptimized (CUDs, CPBDq and CPBDh) UL12 mutants to those with native UL12 sequences demonstrated that deoptimized mutants had significantly lower viral titres on day 2 post-infection.

CPBD of the ICP8 gene reduces ILTV recombination in cell culture

Coinfection of wild-type parent CSW1 with V1-99 resulted in 36% of recovered plaques showing recombinant genotype profiles (Fig. 4), as determined by TaqMan probe assay [30]. No statistical difference in the proportion of recombinant progeny was observed when coinfection was performed using WT.ICP8 (29% recombinants, $P=0.762$) instead of the CSW1 parent. Coinfection of V1-99 with half CPBD ICP8 mutant resulted in significantly fewer recombinant progeny (11%) when compared to CSW1 parent virus ($P=0.049$), but this difference was not significantly different when compared with WT.ICP8 ($P=0.160$), possibly due to insufficient plaque numbers genotyped. Although the use of an assay targeting only five gene regions likely results in an underestimation of recombinant numbers as well as genotype profiles, nine different genotype profiles were detected across the three groups, including those of the parent strains. The most common profile (GT1) was found in 11.8% of isolates (Fig. 5). Parent genotype profiles made up the majority of the isolates tested (75%), with 73.7% corresponding to CSW1. Very low detection of V1-99 parent was recovered in this assay (1.3%), consistent with some previous studies (2.2%) characterizing recombination *in vivo* using these two strains [31, 32].

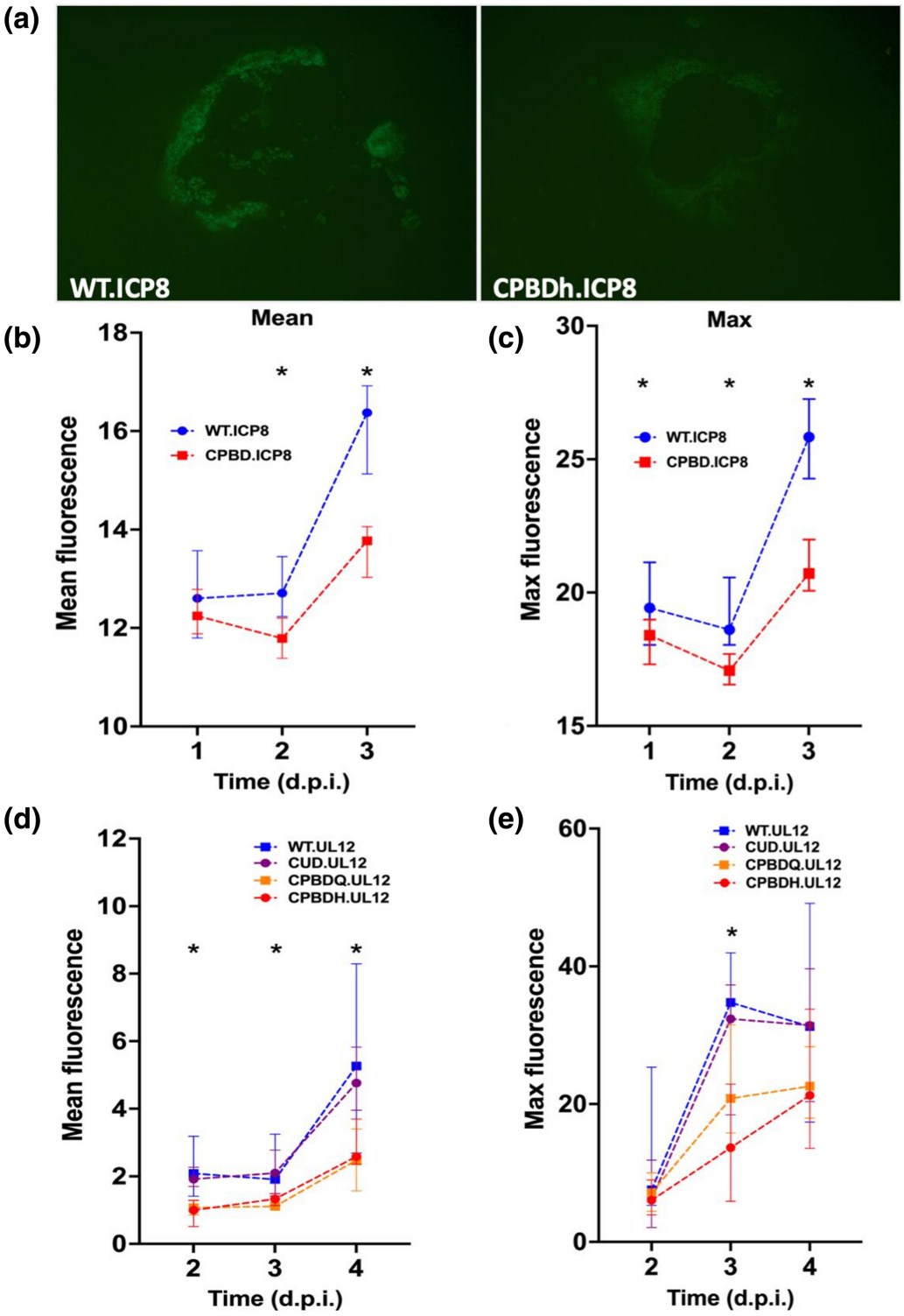

Fig. 2. Comparison of ICP8 and UL12 protein expression in deoptimized mutants to that of viruses containing native ICP8 and UL12 gene sequences, as measured by fluorescence levels. (a) Photomicrographs of green fluorescent plaques induced by WT.ICP8 and CPBDh.ICP8 at 2 d.p.i. of LMH cells, as observed using fluorescence microscopy using a ×10 objective. Line plots showing median and 95% confidence intervals of (b) mean and (c) maximum plaque pixel fluorescence intensity over time of ICP8 GFP-tagged mutants, and (d) mean and (e) maximum plaque pixel fluorescence intensity over time of UL12 GFP-tagged mutants. Asterisks indicate statistical significance. Significant differences were only detected between CPBD mutants and parent viruses; CUD.UL12 virus infected cells did not demonstrate reduced fluorescence.

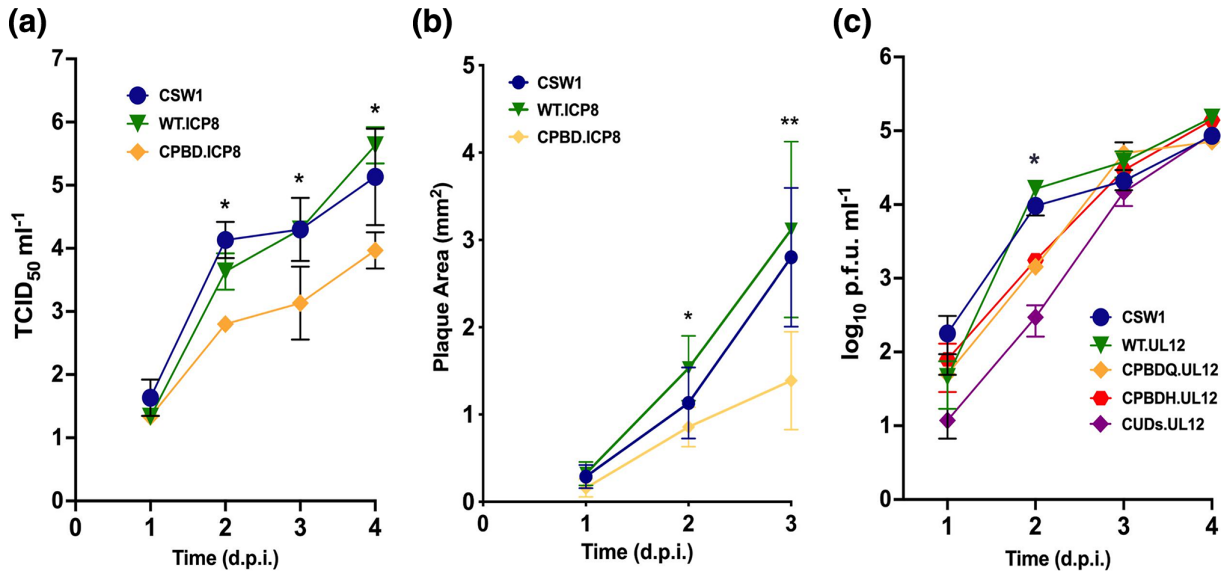

Fig. 3. Comparison of viral replication and cell-to-cell spread characteristics of ICP8 and UL12 mutants and CSW1 parent on LMH cells. (a) Multi-step growth curve and (b) plaque area assay of ICP8 mutants, and (c) multi-step growth curve of UL12 mutants. Mean±SD is shown. Asterisks indicate statistically significant differences (P<0.05) of deoptimized mutants to parent CSW1 virus.

DISCUSSION

The study of the mechanism of ILTV pathogenesis has been hindered by the difficulty to undertake targeted disruption of genes, beyond those not essential for replication in cell culture. Previous attempts to generate ILTV BACs have not been successful [3], unlike for many other diverse herpesviruses where they have been readily available for over 20 years, including for another poultry herpesvirus [42–45]. In this study, two codon deoptimization approaches were applied to assess their efficacy for disrupting, but not completely ablating, the expression of essential genes in ILTV. CUD appeared to be too disruptive a tool to deoptimize large portions of the genes studied, but CPBD was successfully applied to deoptimize at least half of the ILTV ICP8 and UL12 genes. While CPBD viral mutants demonstrated reduced protein expression, neither approach resulted in significantly reduced transcript levels.

This was the first application of CUD and CPBD techniques on ILTV genes, to our knowledge, but CPBD has been previously applied to target three essential genes in another herpesvirus infecting chickens, gallid alphaherpesvirus 2 (Marek's disease herpesvirus, MDV) [21, 23]. As ICP8 is essential for virus replication, and to balance the need for reduction without complete

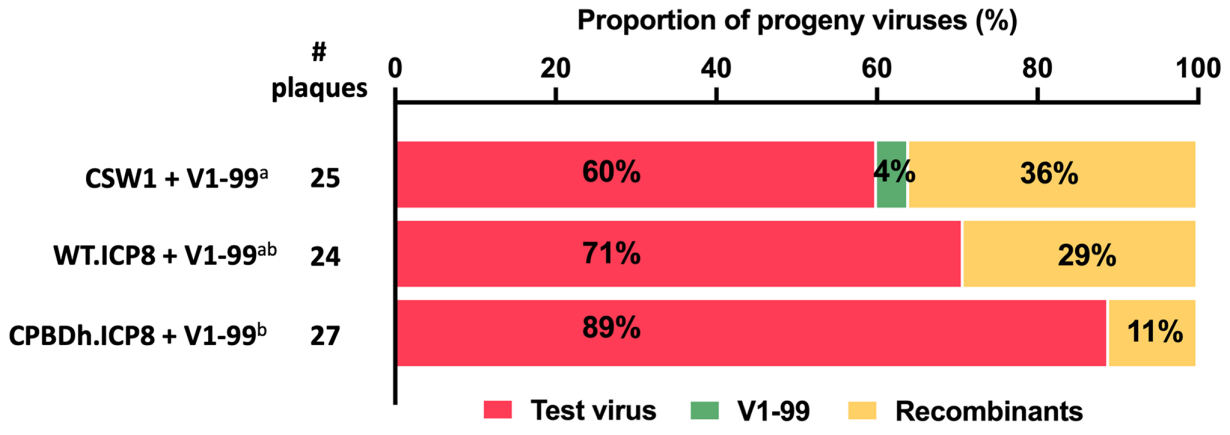

Fig. 4. Genotype proportions of recovered progeny viruses after coinfection of each virus with V1-99 strain. Progeny viruses (n=25 to 27 plaque-purified viruses per group) are categorized as either parent viruses [test viruses (CSW1/WT.ICP8/CPBD.ICP8) or V1-99] or recombinant viruses as determined by TaqMan probe assay [30]. [a,b] lack of significant differences between groups is indicated by the same superscript letter.

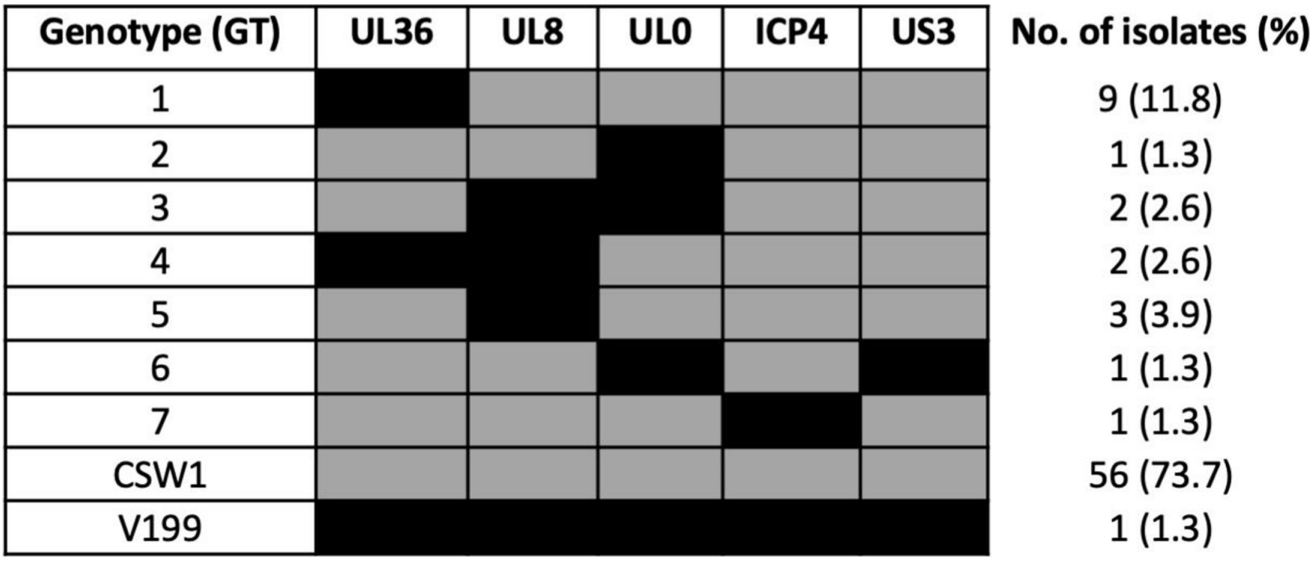

Fig. 5. Genotype profiles produced across the 76 recovered plaques by coinfection experiments.

disruption, only a portion of the gene was chosen for deoptimization by both recoding techniques. Prior studies using CPBD in MDV essential ORFs, as well as comparison of quarter and half CPB deoptimized UL12 in ILTV in this study, did not demonstrate a consistent correlation between the proportion of gene recoded and subsequent degree of downregulation of protein expression. In this study, only the plaque maximum fluorescence intensity measure demonstrated that an increase in the proportion of gene deoptimized proportionally decreased protein expression. This contrasts with what has been observed for some RNA viruses for which this methodology has been more commonly applied [46]. This may be indicative of a higher capacity for large DNA viruses to compensate for translational disruption or perhaps increased redundancy encoded within their genomes compared to smaller RNA viruses.

The successful application of CPBD to generate ILTV mutants with decreased ICP8 and UL12 expression has demonstrated a promising new methodology for the study of these genes and other seemingly important or essential ILTV ORFs. Future studies could use the generated mutants to further define the roles of ILTV ICP8 and UL12 in virus recombination and replication, including their interactions, host responses to infection, and a possible role for ILTV ICP8 in the formation of replication compartments, as has been demonstrated for ICP8 in HSV-1 [47]. In addition, it may be possible to further limit the recombination capacity of ILTV by applying CPBD to both the UL12 and ICP8 genes concurrently. Beyond investigations into ICP8 and UL12, gene-deletion studies have suggested that nuclear protein UL[−1] and glycoprotein D are indispensable for *in vitro* replication [14, 28]. In addition, a mutant in which all of the ILTV-specific ORFs A–E were deleted could not be generated [6]. The functions of these genes may be investigated in future studies using CPBD. There also appear to be ORFs that display essential or quasi-essential properties depending on the parent strain utilized. Construction of gI and gE deletant mutants was not possible using CSW1 [48, 49], but it was possible to severely abrogate or remove them in the A489 strain of ILTV [14]. CPBD could be applied to gI/gE as an alternative to complete deletion in CSW1 to investigate strain to strain variation.

Previous studies on ICP8 and its function in herpesvirus activity have been performed in other viruses by modifying select regions within the protein involved in annealing and observing for reduced rates of replication [25]. This is, to our knowledge, the first study using gene deoptimization approaches to directly investigate the effect of decreased ICP8 expression on both viral replication and recombination. While CPBD of UL12 appears to result (by Western blot) in reduced UL12-specific protein expression, Western blot was not able to detect an obvious reduction in ICP8 expression relative to that of unmodified viral gD, despite reduced levels of fluorescence being detected using microscopy techniques. This may be because the reduction in ICP8 expression was relatively subtle and, thus, only detectable by microscopy and not by semi-quantitative Western blotting. Alternatively, or in addition, the reduced levels of fluorescence detected by microscopy may be related to the reduced levels of viral replication (Fig. 3) that may be induced by even subtle disruption to ICP8 expression. These observations could reflect the essential nature of ICP8 in herpesviruses compared to UL12, which is important, but not essential, for viral replication.

In this study, we were able to demonstrate that reduced ICP8 expression led to a reduced proportion of recombinant progeny *in vitro* relative to the unmodified parent, consistent with the predicted role of ILTV ICP8 in recombination, as well as a consequence of slowed replication overall. Given the importance of recombination in ILTV infection and pathogenicity in

the poultry industry, a vaccine candidate with a reduced ability to recombine could be advantageous. Future *in vivo* studies measuring the incidence of recombination using the CPBDh.ICP8 mutant are indicated to investigate whether the role of ICP8 in recombination is also reflected during coinfection of its natural host. This is turn will help to inform the potential suitability of the CPBDh.ICP8 mutant, or other ICP8-disrupted ILTV mutants, as candidate attenuated vaccines.

Funding information
This work was supported by the Australian Research Council (DP180101417).

Acknowledgements
The authors would like to thank Jawad Sabir for the use of his ILTV gI and gD rat hyperimmune sera, and Professors Glenn Browning and Amir Hadjinoormohammadi for their thoughtful discussions over the course of this project.

Author contributions
P.K.V. designed and performed experiments involving ICP8 viruses and drafted the manuscript. M.A. performed experiments involving UL12 viruses. C.A.H. and J.M.D. devised the experimental design and assisted in statistical analysis and drafting of the manuscript.

Conflicts of interest
The authors declare that there are no conflicts of interest.

References

1. Agnew-Crumpton R, Vaz PK, Devlin JM, O'Rourke D, Blacker-Smith HP, *et al*. Spread of the newly emerging infectious laryngotracheitis viruses in Australia. *Infect Genet Evol* 2016;43:67–73.
2. Lee S-W, Devlin JM, Markham JF, Noormohammadi AH, Browning GF, *et al*. Comparative analysis of the complete genome sequences of two Australian origin live attenuated vaccines of infectious laryngotracheitis virus. *Vaccine* 2011;29:9583–9587.
3. Nadimpalli M. *Genetic manipulation of infectious laryngotracheitis virus by targeted homologous recombination*. Thesis, University of Melbourne, Australia, 2016.
4. Devlin JM, Browning GF, Hartley CA, Kirkpatrick NC, Mahmoudian A, *et al*. Glycoprotein G is a virulence factor in infectious laryngotracheitis virus. *J Gen Virol* 2006b;87:2839–2847.
5. Veits J, Lüschow D, Kindermann K, Werner O, Teifke JP, *et al*. Deletion of the non-essential UL0 gene of infectious laryngotracheitis (ILT) virus leads to attenuation in chickens, and UL0 mutants expressing influenza virus haemagglutinin (H7) protect against ILT and fowl plague. *J Gen Virol* 2003;84:3343–3352.
6. Veits J, Mettenleiter TC, Fuchs W. Five unique open reading frames of infectious laryngotracheitis virus are expressed during infection but are dispensable for virus replication in cell culture. *J Gen Virol* 2003;84:1415–1425.
7. Fuchs W, Wiesner D, Veits J, Teifke JP, Mettenleiter TC. *In vitro* and *in vivo* relevance of infectious laryngotracheitis virus gJ proteins that are expressed from spliced and nonspliced mRNAs. *J Virol* 2005;79:705–716.
8. Fuchs W, Mettenleiter TC. DNA sequence of the UL6 to UL20 genes of infectious laryngotracheitis virus and characterization of the UL10 gene product as a nonglycosylated and nonessential virion protein. *J Gen Virol* 1999;80 (Pt 8):2173–2182.
9. Fuchs W, Mettenleiter TC. The nonessential UL49.5 gene of infectious laryngotracheitis virus encodes an O-glycosylated protein which forms a complex with the non-glycosylated UL10 gene product. *Virus Res* 2005;112:108–114.
10. Fuchs W, Veits J, Helferich D, Granzow H, Teifke JP, *et al*. Molecular biology of avian infectious laryngotracheitis virus. *Vet Res* 2007;38:261–279.
11. Fuchs W, Ziemann K, Teifke JP, Werner O, Mettenleiter TC. The non-essential UL50 gene of avian infectious laryngotracheitis virus encodes a functional dUTPase which is not a virulence factor. *J Gen Virol* 2000;81:627–638.
12. Garcia M, Spatz SJ, Cheng Y, Riblet SM, Volkening JD, *et al*. Attenuation and protection efficacy of ORF C gene-deleted recombinant of infectious laryngotracheitis virus. *J Gen Virol* 2016;97:2352–2362.
13. Helferich D, Veits J, Teifke JP, Mettenleiter TC, Fuchs W. The UL47 gene of avian infectious laryngotracheitis virus is not essential for in vitro replication but is relevant for virulence in chickens. *J Gen Virol* 2007;88:732–742.
14. Pavlova S, Veits J, Mettenleiter TC, Fuchs W. Identification and functional analysis of membrane proteins gD, gE, gI, and pUS9 of infectious laryngotracheitis virus. *Avian Dis* 2013;57:416–426.
15. Schnitzlein WM, Winans R, Ellsworth S, Tripathy DN. Generation of thymidine kinase-deficient mutants of infectious laryngotracheitis virus. *Virology* 1995;209:304–314.
16. Gutman GA, Hatfield GW. Nonrandom utilization of codon pairs in *Escherichia coli*. *Proc Natl Acad Sci* 1989;86:3699–3703.
17. Sharp PM, Li WH. The Codon Adaptation Index – a measure of directional synonymous codon usage bias, and its potential applications. *Nucleic Acids Res* 1987;15:1281–1295.
18. Coleman JR, Papamichail D, Skiena S, Futcher B, Wimmer E, *et al*. Virus attenuation by genome-scale changes in codon pair bias. *Science* 2008;320:1784–1787.
19. Mueller S, Papamichail D, Coleman JR, Skiena S, Wimmer E. Reduction of the rate of poliovirus protein synthesis through large-scale codon deoptimization causes attenuation of viral virulence by lowering specific infectivity. *J Virol* 2006;80:9687–9696.
20. Wang B, Yang C, Tekes G, Mueller S, Paul A, *et al*. Recoding of the vesicular stomatitis virus L gene by computer-aided design provides a live, attenuated vaccine candidate. *mBio* 2015;6:e00237-15.
21. Conrad SJ, Silva RF, Hearn CJ, Climans M, Dunn JR. Attenuation of Marek's disease virus by codon pair deoptimization of a core gene. *Virology* 2018;516:219–226.
22. Eschke K, Trimpert J, Osterrieder N, Kunec D. Attenuation of a very virulent Marek's disease herpesvirus (MDV) by codon pair bias deoptimization. *PLoS Pathog* 2018;14:e1006857.
23. Khedkar PH, Osterrieder N, Kunec D. Codon pair bias deoptimization of the major oncogene meq of a very virulent Marek's disease virus. *J Gen Virol* 2018;99:1705–1716.
24. Schumacher AJ, Mohni KN, Kan Y, Hendrickson EA, Stark JM, *et al*. The HSV-1 exonuclease, UL12, stimulates recombination by a single strand annealing mechanism. *PLoS Pathog* 2012;8:e1002862.
25. Weerasooriya S, DiScipio KA, Darwish AS, Bai P, Weller SK. Herpes simplex virus 1 ICP8 mutant lacking annealing activity is deficient for viral DNA replication. *Proc Natl Acad Sci* 2019;116:1033–1042.
26. Kawaguchi T, Nomura K, Hirayama Y, Kitagawa T. Establishment and characterization of a chicken hepatocellular carcinoma cell line, LMH. *Cancer Res* 1987;47:4460–4464.
27. Lee S-W, Hartley CA, Coppo MJC, Vaz PK, Legione AR, *et al*. Growth kinetics and transmission potential of existing and emerging field strains of infectious laryngotracheitis virus. *PLoS One* 2015;10:e0120282.

28. Nadimpalli M, Lee SW, Devlin JM, Gilkerson JR, Hartley CA. Impairment of infectious laryngotracheitis virus replication by deletion of the UL[-1] gene. *Arch Virol* 2017;162:1541–1548.
29. Devlin JM, Hartley CA, Gilkerson JR, Coppo MJC, Vaz P, *et al*. Horizontal transmission dynamics of a glycoprotein G deficient candidate vaccine strain of infectious laryngotracheitis virus and the effect of vaccination on transmission of virulent virus. *Vaccine* 2011;29:5699–5704.
30. Loncoman CA, Hartley CA, Coppo MJC, Vaz PK, Diaz-Méndez A, *et al*. Development and application of a TaqMan single nucleotide polymorphism genotyping assay to study infectious laryngotracheitis virus recombination in the natural host. *PLoS One* 2017a;12:e0174590.
31. Loncoman CA, Hartley CA, Coppo MJC, Browning GF, Quinteros JA, *et al*. Replication-independent reduction in the number and diversity of recombinant progeny viruses in chickens vaccinated with an attenuated infectious laryngotracheitis vaccine. *Vaccine* 2018;36:5709–5716.
32. Loncoman CA, Hartley CA, Coppo MJC, Vaz PK, Diaz-Méndez A, *et al*. Genetic diversity of infectious laryngotracheitis virus during in vivo coinfection parallels viral replication and arises from recombination hot spots within the genome. *Appl Environ Microbiol* 2017b;83:e01532-17.
33. Jorge DM de M, Mills RE, Lauring AS. CodonShuffle: a tool for generating and analyzing synonymously mutated sequences. *Virus Evol* 2015;1:vev012.
34. Kunec D, Osterrieder N. Codon pair bias is a direct consequence of dinucleotide bias. *Cell Rep* 2016;14:55–67.
35. Pédelacq J-D, Cabantous S, Tran T, Terwilliger TC, Waldo GS. Engineering and characterization of a superfolder green fluorescent protein. *Nat Biotechnol* 2006;24:79–88.
36. Fuchs W, Mettenleiter TC. DNA sequence and transcriptional analysis of the UL1 to UL5 gene cluster of infectious laryngotracheitis virus. *J Gen Virol* 1996;77 (Pt 9):2221–2229.
37. Schneider CA, Rasband WS, Eliceiri KW. NIH Image to ImageJ: 25 years of image analysis. *Nat Methods* 2012;9:671–675.
38. Sabir AJ, Adams TE, O'Rourke D, Devlin JM, Noormohammadi AH. Investigation onto the correlation between systemic antibodies to surface glycoproteins of infectious laryngotracheitis virus (ILTV) and protective immunity. *Vet Microbiol* 2019;228:252–258.
39. Livak KJ, Schmittgen TD. Analysis of relative gene expression data using real-time quantitative PCR and the 2(-Delta Delta C(T)) method. *Methods* 2001;25:402–408.
40. Vaz PK, Motha J, McCowan C, Ficorilli N, Whiteley PL, *et al*. Isolation and characterization of a novel herpesvirus from a free-ranging eastern grey kangaroo (*Macropus giganteus*). *J Wildl Dis* 2013;49:143–151.
41. Flint S, Enquist W, Racaniello V, Skalka A. *Principles of Virology*. 3rd edn. Washington, DC: American Society for Microbiology; 2009.
42. Arii J, Hushur O, Kato K, Kawaguchi Y, Tohya Y, *et al*. Construction of an infectious clone of canine herpesvirus genome as a bacterial artificial chromosome. *Microbes Infect* 2006;8:1054–1063.
43. Arii J, Kato K, Kawaguchi Y, Tohya Y, Akashi H. Analysis of herpesvirus host specificity determinants using herpesvirus genomes as bacterial artificial chromosomes. *Microbiol Immunol* 2009;53:433–441.
44. Schumacher D, Tischer BK, Fuchs W, Osterrieder N. Reconstitution of Marek's disease virus serotype 1 (MDV-1) from DNA cloned as a bacterial artificial chromosome and characterization of a glycoprotein B-negative MDV-1 mutant. *J Virol* 2000;74:11088–11098.
45. Warden C, Tang Q, Zhu H. Herpesvirus BACs: past, present, and future. *J Biomed Biotechnol* 2011;2011:124595.
46. Martínez MA, Jordan-Paiz A, Franco S, Nevot M. Synonymous virus genome recoding as a tool to impact viral fitness. *Trends Microbiol* 2016;24:134–147.
47. Darwish AS, Grady LM, Bai P, Weller SK. ICP8 filament formation is essential for replication compartment formation during herpes simplex virus infection. *J Virol* 2015;90:2561–2570.
48. Devlin JM, Browning GF, Gilkerson JR. A glycoprotein I- and glycoprotein E-deficient mutant of infectious laryngotracheitis virus exhibits impaired cell-to-cell spread in cultured cells. *Arch Virol* 2006a;151:1281–1289.
49. Armat M, Vaz PK, Browning GF, Noormohammadi AH, Hartley CA, *et al*. Construction and characterisation of glycoprotein E and glycoprotein I deficient mutants of Australian strains of infectious laryngotracheitis virus using traditional and CRISPR/Cas9-assisted homologous recombination techniques. *Virus Genes* 2022;58:540–549.